# Multiscale Modeling of Turbulence, Radiation and Combustion Interactions in Turbulent Flames

Michael F. Modest
Department of Mechanical and Nuclear Engineering
Penn State University
University Park, PA 16802
email: mfm6@psu.edu

August 19, 2004

**Abstract**

Traditional modeling of radiative transfer in reacting flows has ignored turbulence–radiation interactions (TRI), due to difficulties caused by their inherent nonlinearities and their vast range of length scales and time scales. The state-of-the-art of modeling TRI is reviewed, and some results are presented, in which TRI are calculated from basic principles from the composition PDF method and from DNS calculations. The results show that, in turbulent jet flames, TRI are always of great importance, and that they are dominated by the correlation between the absorption coefficient and the radiative Planck function.

# Introduction

Most fires as well as commercial combustion processes, such as boilers, internal combustion engines, gas turbines, etc., involve high temperatures and, therefore, thermal radiation usually contributes a significant fraction to the overall heat transfer rates. At the same time, the vast majority of these combustion applications occur under turbulent conditions, which is known to enhance heat transfer. Radiation, chemical kinetics and turbulence individually are among the most challenging fundamental and practical problems of computational science and engineering, due to their inherent nonlinearities and their vast range of length scales and time scales. In turbulent combustion, these phenomena are coupled in interesting and highly nonlinear ways, leading to entirely new classes of interactions. In much the same way as convection is aided by turbulence, so is radiation, which in the presence of chemical reactions may increase several fold due to turbulence interactions. While coupling between turbulence and chemistry has received a great deal of attention over the years [1, 2], turbulence-radiation interaction (hereafter TRI) has until recently been ignored by virtually all investigations due to its extreme complexity, even though its importance has been widely recognized [3–7]. Preliminary and state-of-the-art calculations have shown that TRI always increases the heat loss from a flame, and that this additional heat loss can reach 60% of the total and more, leading to a reduction in the local gas temperature of 200° C or more. Therefore,

in many turbulent flames accurate prediction of radiation and TRI can be expected to be at least as important as accurate modeling of combustion rates and turbulence-chemistry interaction. It is a well-known fact that standard CFD codes can solve the turbulent reacting flow equations only on a time-averaged basis or with filtered length scales, while all subgrid fluctuations need to be modeled. If turbulence-radiation interactions are to be considered, this will result in many unclosed terms, which need to be modeled. Traditional moment methods cannot obtain closure, because too many additional partial differential equations need to be modeled and solved simultaneously, generally exceeding the power of current computers [8]. This, together with the fact that accurate radiation modeling even in the absence of TRI is a daunting task, has prompted the vast majority of researchers to use simplistic radiation models and/or radiation calculations based on mean temperature and concentration fields [9]. On the other hand, experimental evidence has shown that mean radiative quantities in turbulent combustion tend to differ significantly from those based on mean scalar values, and that experimentally measured radiative fluxes can be two times or more larger than those predicted from mean values [10].

In early numerical work the $T^4$-dependence of gray radiation was expanded into a Taylor series, showing that strong temperature fluctuations can significantly enhance radiative emission (known as *temperature self-correlation*) [6, 11, 12]. In a more sophisticated approach Pearce and Varma [13] calculated the TRI in a $CO_2$ band by breaking up a path into statistically independent segments, using two-point exponential correlation functions. This approach was adopted and further developed by Faeth et al. [10] and Chan and Chern [14]. Similar line-of-sight calculations have been carried out also by McDonough and Mengüç [15,16], using chaotic map theory to model scalar fluctuations.

Perhaps the first calculation of a complete combustion problem considering TRI is that by Song and Viskanta [5], who investigated a turbulent premixed flame inside a two-dimensional furnace. Using a standard $k$–$\varepsilon$ model for fluid flow, they achieved closure by using an assumed probability density function (PDF) for the fluctuations of temperature and species concentrations. Similar approaches were used by Gore et al. [17] and by Hartick et al. [18]. Assumed PDF's vastly simply the overall complexity of the problem by eliminating the need for subgrid models. For that reason all but a handful of researchers to date have used the assumed PDF approach, using various types of PDF's, as well as different levels of sophistication for the chemical kinetics and thermal radiation submodels. For example, Ripoll [19] outlines how TRI can be evaluated using the simple $M_1$-radiation solver (a somewhat more sophisticated derivative of the popular spherical harmonic $P_1$-method) together with Gaussian assumed PDFs. A more advanced approach was taken by Coelho et al. [20] to model Flame D from the International Workshop on Measurement and Computation of Turbulent Nonpremixed Flames [21], for which experimental data are posted on a website. They used a Reynolds stress model for turbulence modeling, the laminar flamelet model for combustion, the discrete ordinates method as radiation solver, together with the SLW model for nongray combustion gas properties, and the assumed PDF's of Song and Viskanta [5] for the TRI.

Resolution or modeling of the subgrid scales requires another level of sophistication. While traditional moment methods appear unsuitable for accurate TRI evaluation, they can be employed for more approximate calculations. For example, Snegirev [22] reduced the TRI term to an expression requiring knowledge of two model constants plus the temperature variance, $\overline{T'^2}$, for which a transport equation is solved. Using the $k$–$\varepsilon$ model for the turbulent flow, a three-reaction combus-

tion scheme together with the eddy break-up model, soot production from empirical correlations and a weighted-sum-of-gray-gases (WSGG) and Monte Carlo method for radiation, he investigated the TRI in large turbulent propane diffusion flames, and also for liquid acetone pool fires. Comparison with experiments [23] shows that neglecting TRI results in an underprediction of the flames' radiant fraction by about 50%. Adjusting his TRI model constants Snegirev was able to make reasonably accurate predictions for a range of flames.

Calculating the probability density function of dependent variables, rather than using assumed values, is generally done by one of the so-called PDF methods. These methods have the unique feature that many nonlinear terms can be treated exactly, such as chemical source terms [24]. For that reason they have been widely used in the modeling of reacting flow (generally neglecting radiation altogether, or treating it with the simple optically-thin approximation) [25–27]. Mazumder and Modest [28] recognized that the radiative source term (including TRI) is mathematically equivalent to the chemical source term, provided the usually very reasonable *optically-thin fluctuation approximation* (OTFA) is made (explained in detail in the next section). They used the velocity-composition joint PDF method, together with a single-step Arrhenius combustion model, and the $P_1$-approximation combined with the WSGG method for radiation, to model a methane-fuelled bluff body combustor. In this first study to determine TRI from basic principles they found TRI to increase radiative heat loss rates by about 40%.

While the velocity-composition PDF method avoids the modeling of velocity fluctuations and time scale information, it adds mathematical complexities and contributes to stability problems. It has, therefore, become popular to decouple chemistry from fluid mechanics by using a hybrid finite volume (FV)–composition PDF method. The momentum and continuity equations are solved using a Eulerian grid-based method (RANS, LES, etc.), while the joint composition PDF is solved to obtain scalar mean fields and their turbulence moments [27, 29]. The first to use this method for the study of TRI were Li and Modest [30, 31]. They modeled axisymmetric methane jet diffusion flames, using a standard $k$–$\varepsilon$ model for the flow field, and for radiation the simple $P_1$-approximation together with a state-of-the-art spectral model for combustion gases, the full-spectrum $k$-distribution method (FSK) [32]. In their first work they considered a simple jet using fast chemistry assessing the importance of several TRI terms [30], while in the second study a single-step Arrhenius rate was used to systematically study the TRI in Flame D as well as a family of larger flames extrapolated from Flame D [31]. They noted that among the various TRI interactions the correlation between absorption coefficient and Planck function is the most important, especially for strongly nongray combustion gases.

In a very similar recent study Tessé et al. [33] considered a sooty turbulent ethylene jet diffusion flame. They also used the $k$–$\varepsilon$ model for the flow field together with the composition PDF method. However, they employed a full chemistry model (119 reactions, plus a five-parameter soot model), and radiation rates were calculated with a photon Monte Carlo method, using a narrow-band correlated-$k$ approach for properties (equivalent to FSK). They also found that radiative heat loss rates increase 25-40% due to TRI (the lesser amount in the presence of essentially-gray soot). Due to the use of the Monte Carlo radiation solver their study is the only one to date for a complete flame that did not require the optically-thin fluctuation approximation. Coelho [34] showed that OTFA can be relaxed for simple line-of-sight calculations by using the semi-causal model of Chan and Pan [35]. They showed that use of OTFA is justified for Flame D; however, since that flame is rather small and optically thin, this was very much expected.

Like traditional moment closure models, PDF methods suffer from unclosed terms, which

need to be modeled. Thus, truly accurate predictions can only come from a model that resolves all disparate length and time scales, i.e., from direct numerical simulation (DNS). A first attempt to resolve all TRI terms in a one-dimensional premixed flame has been made by Wu et al. [36, 37]. They considered a single-step Arrhenius rate equation and assumed the medium's absorption coefficient to be gray and spatially varying. The radiative heat source was determined using a high-order photon Monte Carlo scheme (of order commensurate with the underlying DNS code). Their results confirm previous data on the importance of TRI and shed important light on the interactions neglected through the use of OTFA.

Since use of the composition PDF method appears most promising for the prediction of TRI effects in turbulent flames with their vastly varying length and time scales, the method will be reviewed in some detail in the following sections. Pertinent results from the study by Li and Modest [31] will be reviewed and extended. Finally, a brief discussion will be given how TRI can be evaluated without modeling from DNS calculations, reviewing and extending the work of Wu et al. [36, 37].

# Mathematical Formulation

## Turbulence-Radiation Coupling.

In turbulent, reacting flows conventional averaging (also known as Reynolds averaging) and mass-weighted averaging (also called Favre averaging) are used to formulate the governing equations for mean velocities and scalars (i.e., enthalpy $h$ or temperature $T$, and species concentrations $\underline{Y}$). For example, for low Mach number flows the energy equation may be written as [38]:

$$\langle\rho\rangle\frac{\partial\tilde{h}}{\partial t}+\langle\rho\rangle\tilde{u}_i\frac{\partial\tilde{h}}{\partial x_i}-\frac{\partial\langle p\rangle}{\partial t}=\frac{\partial}{\partial x_i}\left[\Gamma_T\frac{\partial\tilde{h}}{\partial x_i}\right]+\langle S^R\rangle, \tag{1}$$

where $h$ is the absolute enthalpy of the mixture, $\Gamma_T$ is the turbulent diffusivity, and $\left\langle S^R\right\rangle$ is the source term due to thermal radiation; conventional averages are denoted by angle brackets, while Favre averages have a tilde over them. In the total enthalpy formulation the temperature $T$ is contained implicitly in the absolute enthalpy, defined as

$$h=\sum Y_i h_i=\sum Y_i[h_{o,i}+\int c_{p,i}(T)dT], \tag{2}$$

where $Y_i$ and $h_i$ are mass fraction and absolute enthalpy of specie $i$ in the mixture, $h_{o,i}$ is the enthalpy of formation of specie $i$, and $c_{p,i}$ is its specific heat. Note that in the absolute enthalpy formation the heat source due to chemical reactions is contained within the enthalpy of formation. Similar to conduction, thermal radiation traveling through a small volume may lead to a local source or sink of radiative energy, i.e., [39]

$$S^R=-\nabla\cdot\underline{q}^R=\int_0^\infty\kappa_\eta\left(G_\eta-4\pi I_{b\eta}\right)d\eta,\ G_\eta=\int_{4\pi}I_\eta d\Omega \tag{3}$$

where $\underline{q}^R$ denotes the radiative flux vector, $\kappa_\eta(p,T,\underline{Y})$ is the spectral absorption coefficient of the mixture, $I_\eta$ is the spectral radiative intensity, $G_\eta$ is direction-integrated intensity (or incident radiation), and $I_{b\eta}$ is the spectral blackbody intensity (also called Planck function). The subscript $\eta$

indicates a spectrally varying quantity, and $d\Omega$ denotes solid angle. Physically, the radiative source of Eq. (3) may be interpreted as the difference between absorbed incoming and emitted radiation. The radiative intensity must be found from the radiative transfer equation (RTE), which for an absorbing, emitting but not scattering medium is [39]

$$(\hat{\mathbf{s}} \cdot \nabla) I_\eta = \kappa_\eta (I_{b\eta} - I_\eta), \tag{4}$$

where $\hat{\mathbf{s}}$ is a unit direction vector. While the RTE is a five-dimensional partial differential equation (3 spatial and 2 directional coordinates), it is usually sufficient to use its quasi-steady form, since the time constant for radiative transport within a 1m enclosure is of the order of a few nanoseconds. This is considerably faster than the time constants encountered in turbulence or even the fastest chemical reactions. Before substituting $S^R$ into Eq. (1), Eqs. (3) and (4) must be time-averaged, leading to

$$\langle S^R \rangle = \int_0^\infty \left[ \int_{4\pi} \langle \kappa_\eta I_\eta \rangle d\Omega - 4\pi \langle \kappa_\eta I_{b\eta} \rangle \right] d\eta = \int_0^\infty \left[ \left\langle \kappa_\eta G_\eta \right\rangle - 4\pi \langle \kappa_\eta I_{b\eta} \rangle \right] d\eta, \tag{5}$$

$$(\hat{\mathbf{s}} \cdot \nabla) \langle I_\eta \rangle = \langle \kappa_\eta I_{b\eta} \rangle - \langle \kappa_\eta I_\eta \rangle. \tag{6}$$

The time averaged terms $\langle \kappa_\eta I_\eta \rangle$ and $\langle \kappa_\eta I_{b\eta} \rangle$ have a strong, nonlinear dependence on temperature and species concentrations and, therefore, cannot be evaluated from mean values for $\left\langle I_\eta \right\rangle$ and the scalars $\tilde{h}$ and $\underline{\tilde{Y}}$. The differences between these terms,

$$\langle \kappa_\eta I_\eta \rangle - \kappa_\eta \left( \langle p \rangle, \tilde{h}, \underline{\tilde{Y}} \right) \left\langle I_\eta \right\rangle \quad \text{and} \quad \langle \kappa_\eta I_{b\eta} \rangle - \kappa_\eta (\langle p \rangle, \tilde{h}, \underline{\tilde{Y}}) I_{b\eta}(\tilde{h}) \tag{7}$$

constitute the turbulence-radiation interactions. Since the *absorption coefficient-intensity correlation*, $\langle \kappa_\eta I_\eta \rangle$, and *absorption coefficient-Planck function correlation*, $\langle \kappa_\eta I_{b\eta} \rangle$, cannot be expressed in terms of scalar means, these terms in the governing equations must be modeled or calculated independently. The TRI correlations can be placed into two different groups: (a) correlations that can be calculated directly or indirectly from scalars modeled in the composition PDF of the following section ($h$ and $\underline{Y}$), and (b) those that cannot. The correlation $\langle \kappa_\eta I_{b\eta} \rangle$ belongs to group (a), since both $\kappa_\eta$ and $I_{b\eta}$ depend only on temperature and species concentrations.

The correlation $\langle \kappa_\eta I_\eta \rangle$, on the other hand, belongs to group (b), since radiative intensity is not one of the scalars modeled in the composition PDF. However, as recognized by Kabashnikov and Myasnikova [40], the fluctuation of local intensity are governed by points far away and are only weakly correlated with the fluctuations of the local absorption coefficient, if the mean free path for radiation is much larger than the turbulence length scale. Thus, within the framework of the *optically thin eddy approximation* or *optically thin fluctuation assumption* (OTFA), we have

$$\langle \kappa_\eta I_\eta \rangle \simeq \langle \kappa_\eta \rangle \langle I_\eta \rangle \quad \text{if} \quad \kappa_\eta l < 1, \tag{8}$$

where $l$ is an appropriate turbulence length scale. The *absorption coefficient self-correlation* $\langle \kappa_\eta \rangle$ is still a nonlinear average but belongs to group (a). The validity of OTFA depends on eddy size distribution and the absorption coefficient of the mixture. Hartick et al. [18] have shown that in combustion gases OTFA may not be valid over very small parts of the spectrum (e.g., parts of the strong $4.3\mu m$ $CO_2$ band), but that their effect on overall results is negligible. Similarly, Coelho [34] showed OTFA to be valid for the modeling of Flame D. On the other hand, in strongly sooting

flames the absorption coefficient may be very large over substantial parts of the spectrum and OTFA may be violated. For the remainder of this paper we will only consider nonsooting flames and, for the most part, will assume OTFA to be valid. It is important to note that, after invoking OTFA, evaluation of the averaged radiation source term becomes mathematically equivalent to the evaluation of the chemical reaction source term. Thus any method devised for the averaging of chemical sources is immediately applicable to the determination of TRI.

## The Joint Composition PDF Method

In the joint composition PDF method the composition (or scalar) variables are assumed to be random variables and the transport of their probability density function is calculated, rather than the transport of the scalars themselves or their moments. Once the PDF has been determined, the means of any quantity $Q$, as long as it is a function of the scalar field $\underline{\phi} \equiv (Y_1, Y_2, ..., h)$ only (such as chemical source term, Planck function, absorption coefficient, etc.), can be evaluated directly from the PDF as

$$\langle Q \rangle = \int_0^\infty f(\underline{\psi}) Q(\underline{\psi}) d\underline{\psi}. \tag{9}$$

In this equation, $\underline{\psi}$ represents the composition space variable, $\underline{\psi} \equiv (\psi_1, \psi_2, \cdots, \psi_s)$, and $f(\underline{\psi})$ is defined to be the probability density of the compound event $\underline{\phi} = \underline{\psi}$ (i.e., $\phi_1 = \psi_1, \phi_2 = \psi_2, \cdots, \phi_s = \psi_s$), so that,

$$f(\underline{\psi}) d\underline{\psi} = \text{Probability}(\underline{\psi} \le \underline{\phi} < \underline{\psi} + d\underline{\psi}). \tag{10}$$

The composition PDF, $f(\underline{\psi})$, defined informally by Eq. (10), is the simplest form of the PDF methods, since it carries information only about the scalar variables, $\underline{\phi}$. Also, it governs the probability distribution only at a single point. However, since it contains all of the statistical information about the scalars, its determination is in many ways more useful than that of the mean values.

In a general turbulent reactive flow, the composition PDF is also a function of space, $\underline{x}$, and time, $t$. The transport equation for the composition PDF has been derived by Pope for nonradiating reactive flows [24]. For radiating reactive flows, the transport equation for the mass density composition PDF, $\mathscr{F}(\underline{\psi}, \underline{x}, t) = \rho(\underline{\psi}, \underline{x}, t) f(\underline{\psi}, \underline{x}, t)$, can be similarly derived, leading to

$$\begin{aligned} \frac{\partial \mathscr{F}}{\partial t} + \frac{\partial}{\partial x_i}[\tilde{u}_i \mathscr{F}] + \frac{\partial}{\partial \psi_\alpha}[S_\alpha^{\text{chem}}(\underline{\psi}) \mathscr{F}] \;=\; & -\frac{\partial}{\partial x_i}\left[\left\langle u_i'' \,\middle|\, \underline{\psi} \right\rangle \mathscr{F}\right] \\ & + \frac{\partial}{\partial \psi_\alpha}\left[\left\langle \frac{1}{\rho}\frac{\partial J_i^\alpha}{\partial x_i} \,\middle|\, \underline{\psi} \right\rangle \mathscr{F}\right] - \frac{\partial}{\partial \psi_\alpha}\left[\left\langle S^R \,\middle|\, \rho \,\middle|\, \underline{\psi} \right\rangle \mathscr{F}\right], \end{aligned} \tag{11}$$

where $i$ and $\alpha$ are summation indices in physical space and composition space, respectively. The notation of $\langle A \,|B\rangle$ is the expectation of the conditional probability of event $A$, given that event $B$ occurs.

On the left-hand side of Eq. (11), the first two terms represent the rate of change of the PDF when following the Favre-averaged mean flow, and the third term is the transport of the PDF in composition space by chemical reactions. These processes are accounted for exactly. In contrast, the terms on the right-hand side need to be modeled. The first term on the right represents transport in physical space due to turbulent convection. Since the joint composition PDF contains no information on velocity, the conditional expectation of $\langle u_i'' | \underline{\psi} \rangle$ needs to be modeled. Generally, a

gradient-diffusion model with information supplied for the turbulent flow field by a flow solver is employed [24],

$$-\langle u_i^{''}|\psi\rangle\mathscr{F} \simeq \Gamma_T \frac{\partial \mathscr{F}}{\partial x_i},\ \Gamma_T = \frac{c_\mu \langle\rho\rangle k^2}{\sigma_\phi \varepsilon}, \tag{12}$$

where $\Gamma_T$ is the turbulent diffusivity estimated by *ad hoc* turbulent closures [24], where $k, \varepsilon, c_\mu$ and $\sigma_\phi$ are, respectively, the Favre-averaged turbulent kinetic energy, Favre-averaged dissipation rate of turbulent kinetic energy, a modeling coefficient in a standard two-equation $k$–$\varepsilon$ turbulence model, and the turbulent Schmidt or Prandtl number. Such gradient transport models are, of course, approximate and more accurate models may be employed when called for.

The second term on the right-hand side of Eq. (11) represents transport in scalar space due to molecular mixing. This term has been found to be crucial and many mixing models such as the interaction-by-exchange-with-the-mean (IEM) model [41], also known as the linear mean square estimation (LMSE) model, and Pope's particle-pairing model [24] have been proposed. Good discussions on the current development of molecular mixing models may be found in [42–44]. Usually, the simple IEM model is used, which states

$$\left\langle \frac{1}{\rho}\frac{J_i^\alpha}{\partial x_i}\middle|\underline{\psi}\right\rangle \simeq \frac{1}{2}C_\phi \omega(\psi_\alpha - \tilde{\phi}_\alpha), \tag{13}$$

where $C_\phi$ is a model constant and $\omega$ is the mixing frequency, which is calculated using the $k$–$\varepsilon$ model, i.e., $\omega = \varepsilon/k$.

The third term on the right-hand side of Eq. (11) represents the contribution from thermal radiation,

$$-\frac{\partial}{\partial\psi_s}\left[\left\langle S^R/\rho\middle|\underline{\psi}\right\rangle \mathscr{F}\right] = \frac{\partial}{\partial\psi_s}\left[\left\langle \int_0^\infty \kappa_\eta(4\pi I_{b\eta} - G_\eta)d\eta/\rho\middle|\underline{\psi}\right\rangle \mathscr{F}\right]. \tag{14}$$

The first term in the integral on the right-hand side represents radiative emission and can be evaluated exactly. The second term can be closed by adopting the OTFA, leading to

$$-\frac{\partial}{\partial\psi_s}\left[\left\langle S^R/\rho\middle|\underline{\psi}\right\rangle \mathscr{F}\right] = \frac{\partial}{\partial\psi_s}\left[\left(\int_0^\infty 4\pi\kappa_\eta I_{b\eta}d\eta - \int_0^\infty \kappa_\eta\langle G_\eta\rangle d\eta\right)\mathscr{F}/\rho\right]. \tag{15}$$

The composition PDF can, in principle, be solved by traditional finite volume means, as was done, for example, by Janicka et al. [45]. However, in all but the simplest combustion scenarios the PDF is a differential equation of very high order (three spatial variables and $s$ composition variables, i.e., $s-1$ species concentration as well as enthalpy), making finite volume solutions impractical. Instead, the PDF is usually solved stochastically, converting the partial differential equation into Lagrangian equations for large numbers of notional particles, which are tracked with a Monte Carlo scheme [24, 29]. For the modeled mass density PDF function, Eq. (11), the corresponding particle equations for location, $\underline{x}$, and scalar quantities, $\underline{\phi}$ are governed by the following stochastic

differential equations:

$$d\underline{x}^\star(t) = [\underline{\tilde{u}} + \nabla\Gamma_T/\langle\rho\rangle]_{\underline{x}^\star(t)}dt + [2\Gamma_T/\langle\rho\rangle]^{1/2}_{\underline{x}^\star(t)}d\underline{W}, \tag{16}$$

$$d\phi^\star_\alpha(t) = S^{\text{chem}\star}_\alpha dt - \frac{C_\phi}{2}\frac{\varepsilon}{k}(\phi^\star_\alpha - \tilde{\phi}_\alpha)dt - \delta_{\alpha s}\int_0^\infty \kappa_\eta(4\pi I_{b\eta} - \langle G_\eta\rangle)d\eta\frac{dt}{\rho^\star}, \quad \alpha = 1, \cdots, s. \tag{17}$$

Here the variables with an asterisk refer to the values of a Lagrangian particle and $\underline{W}$ is an isotropic vector Wiener process, which is used to mimic the turbulent diffusion process. $\delta_{\alpha s}$ is Kronecker's delta, i.e., the radiation source is present only in the stochastic energy equation for $\phi_s = h$. The composition PDF, whether in its deterministic form, Eq. (11), or its stochastic form, Eqs. (16) and (17), only evaluates the scalars $\phi_\alpha$, i.e., mass fractions and enthalpy. Pressure, velocity field and, in the presence of radiation, the mean incident radiation $\langle G_\eta \rangle$ must be supplied from an external solver, for example, standard commercial CFD packages, such as Fluent [46]. Both codes then form an iterative loop, with the CFD code calculating (and feeding to the PDF code) the flow field and $\langle G_\eta \rangle$, while the PDF module calculates the scalars (including all necessary turbulent moments such as chemical and radiative sources); the PDF code then feeds chemistry-induced density changes back to the CFD solver. Good implementation of such hybrid FV-PDF schemes use common grids for both solvers in order to resolve sharp gradients in regions of chemical reactions. This requires time step splitting and particle splitting and combination techniques, preferentially placing and tracking particles in regions of strong gradients [27, 29–31, 47].

## Chemical Reaction Submodel

One of the great strengths of PDF methods is their ability to calculate nonlinear source terms exactly, without approximation (chemical reaction sources and – within the framework of OTFA – the radiative source). The chemical source term is reduced to a set of ordinary differential equations; however, their stiff nature make the calculations very expensive. A typical PDF simulation may track $10^6$ particles for perhaps 1000 time steps, thus requiring $10^9$ source term integrations: using full kinetics would be computationally intractable. Therefore, even PDF simulations generally use relatively simple kinetics, such as a single-step skeletal mechanism with an Arrhenius reaction rate (such as the reaction rate for methane given by Westbrook and Dryer [48], which was used for the results shown in later sections). If sophisticated kinetics are considered, acceleration techniques must be employed [27], such as ISAT (in situ adaptive tabulation) [49] or DOLFA (Database for On-Line Function Approximation) [50, 51].

## Thermal Radiation Submodel

Accurate determination of radiative heat fluxes is always an extremely challenging task, for one because of the five-dimensionality of the RTE, Eq. (4), and also because of the strong spectral variation of radiative properties, in particular those of combustion gases. A detailed discussion on the RTE solution techniques and on state-of-the-art spectral models may be found in the book by Modest [39]. Most modern CFD packages have a decent array of RTE solvers embedded, such as

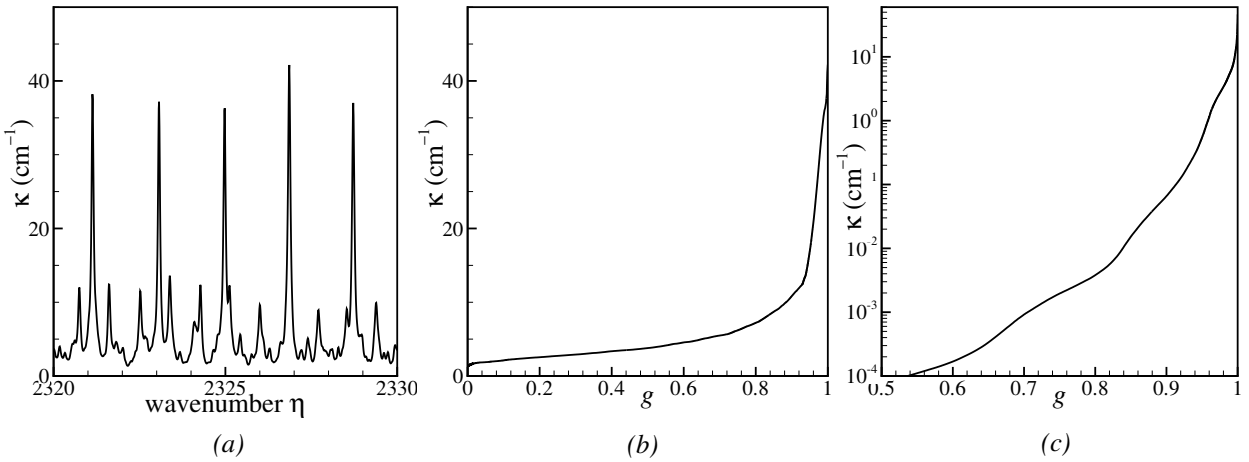


Figure 1. (a) Absorption coefficient for part of the 4.3 $\mu$m $CO_2$ band; (b) $k$-distribution of the absorption coefficient for the same part of the 4.3 $\mu$m $CO_2$ band; (c) full spectrum $k$-distribution; all for pure $CO_2$ at $T = 1000$ K and $p = 1$ bar

the popular discrete ordinates method (DOM, of arbitrary order $S_N$) and the spherical harmonics method (low order, $P_1$) [39]. However, none have embedded, or allow to be attached, an accurate nongray spectral technique. State-of-the-art investigations for radiation in combustion systems tend to use global spectral models, which provide a reasonable compromise between simplicity and accuracy. The simplest (and oldest) global model is the weighted sum of gray gases (WSGG) [52, 53], which employs fairly dated experimental data for properties. More modern methods are the spectral line-based WSGG (SLW) method [54, 55] or the equivalent absorption distribution function approach [56, 57]; both methods use modern spectroscopic databases, such as HITRAN [58] or HITEMP [59] for the determination of WSGG properties. The most advanced global model is the full-spectrum $k$-distribution approach for narrow spectral bands extended to the full spectrum. Modest [32, 39, 60] has shown that the SLW and ADF are low-level implementations of the FSK method.

In narrow band $k$-distributions the strongly oscillating absorption coefficient is reordered into a monotonically increasing function. Realizing that every identical value for absorption coefficient produces an identical intensity, the absorption coefficient may be reordered to avoid repetitive calculations. An example of this reordering is shown in Fig. 1*a* and *b*, depicting a small part of the 4.3$\mu$m $CO_2$ band for pure $CO_2$ at 1000K, 1bar. Modest and Zhang [60] have shown that the $k$-distribution can be extended to the full spectrum by weighting the distribution with the local Planck function. Fig. 1*c* shows such a $k$-distribution for the entire spectrum with more than 1 million spectral lines, indicating that such distributions have similar smoothness as their narrow band counterparts but span several orders of magnitude for $k$ and are compressed toward large values of $g$ (because of a gas' "spectral windows" across much of the spectrum). This leads to a reordered RTE

$$\frac{dI_g}{ds} = k(\underline{\phi}, g)\Big[a(T, g)I_b - I_g\Big], \tag{18}$$

where

$$a(T, g) = \frac{f(T, k)}{f(T_o, k)} = \frac{dg(T, k)}{dg(T_o, k)}, \tag{19}$$

is a spectral stretching factor between local temperature $T$ and reference temperature $T_o$, and

$$f(T,k) = \frac{1}{I_b(T)} \int_0^\infty I_{b\eta}(T)\delta(k-\kappa_\eta)d\eta, \tag{20}$$

$$g(T,k) = \int_0^k f(T,k)dk = \frac{1}{I_b(T)} \int_0^\infty I_{b\eta}(T)H(k-\kappa_\eta)d\eta \tag{21}$$

are the full-spectrum $k$-distribution and cumulative $k$-distribution, respectively. Here $\delta$ is the Dirac-delta function and $H$ is Heaviside's unit step function. In media without too extreme nonhomogeneities the FSK methods (in its scaled and correlated versions for nonhomogeneous media [61]) rival LBL calculations in accuracy, but at about 1/100,000 the computational cost.

The spectrally integrated intensity is then obtained by integration over $g$-space (usually enacted by Gaussian quadrature with $M$ = 8-10 quadrature points),

$$I = \int_0^\infty I_\eta d\eta = \int_0^1 I_g dg \simeq \sum_{m=1}^{M} w_m I_m, \tag{22}$$

where the $w_m$ are Gaussian quadrature weights. While any solver can be used with the FSK methods and for the evaluation of TRI [i.e., Eq. (18) is readily averaged within the limitations of OTFA], the simple $P_1$-method will be invoked for the results of the following sections: this results in simple Helmholtz equations, which are easily implemented in standard CFD packages as "additional scalars." Thus [39]

$$\nabla \cdot \left[ \frac{1}{3\langle k_m \rangle} \nabla \langle G_m \rangle \right] = \langle k_m \rangle \langle G_m \rangle - 4\pi \langle k_m a_m I_b \rangle \,;\; m = 1, ...M, \tag{23}$$

from which the radiative source is obtained as

$$\left\langle S^R \right\rangle = -\sum_{m=1}^{M} \langle S \rangle w_m \left[ 4\pi \langle k_m a_m I_b \rangle - \langle k_m \rangle \langle G_m \rangle \right]. \tag{24}$$

# Turbulence-Radiation Interactions in Diffusion Jet Flames

Turbulent, nonpremixed jet flames have been investigated by Li and Modest to study various TRI effects [62–65]. Besides the type of fuel the flame structure depends on jet diameter, $d_j$, jet velocity $u_j$, coflow air velocity, $u_{\text{air}}$, and various properties of the reacting species. It is expected that general flame behavior is largely governed by four nondimensional parameters, namely Reynolds number Re, flame optical thickness $\tau_{\text{flame}}$, Damköhler number, Da, and Froude number, Fr. The Reynolds number is always important in turbulent flows; in a jet flow Re is generally defined based on the jet diameter and velocity as

$$\text{Re} \equiv \frac{\rho u_j d_j}{\mu}, \tag{25}$$

where $\rho$ and $\mu$ are density and viscosity of fuel mixture at the inlet. The flame's optical thickness governs the level of radiative heat loss from the flame. While this parameter is a local, directional and spectral quantity, a nominal optical thickness may be defined as

$$\tau_{\text{flame}} \equiv \kappa_P L_{\text{flame}}, \tag{26}$$

where $\kappa_P$ is an average Planck-mean absorption coefficient and $L_{\text{flame}}$ is the length, which is approximately a linear function of jet diameter [66], here estimated as $L_{\text{flame}} = 40 d_j$. An important nondimensional parameter comparing time scales in the flame is the Damköhler number

$$\text{Da} \equiv \frac{t_{\text{flow}}}{t_{\text{reaction}}}, \tag{27}$$

where the flow time scale can be estimated from $t_{\text{flow}} = d_j/u_j$, while the chemical reaction time scale can be estimated from the reaction rate equation (here taken as a one-step Arrhenius rate). Finally, buoyancy effects are characterized by the Froude number, for turbulent flames often set as [66]

$$\text{Fr} \equiv \frac{u_j f_s^{3/2}}{\left(\frac{\rho_j}{\rho_{\text{air}}}\right)^{1/4} \left[\frac{\Delta T_f}{T_\infty} g d_j\right]^{1/2}} \tag{28}$$

where $f_s$ is stoichiometry and $\Delta T_f$ is a characteristic temperature rise resulting from combustion.

Twelve different flames were studied, all using the same fuel and general setup as Sandia Flame D, for which Re $= 22,400$, $\tau_{\text{flame}} = 0.237$, $Da = 317.5$ and $Fr \to \infty$. Different types of flames where generated from the Flame D baseline, by changing only one of the nondimensional parameters while keeping the others constant. This was achieved by varying jet diameter $d_j$, jet velocity $u_j$, chemical reaction rate preexponential factor $A$ and/or gravitational acceleration $g$. For example, to double Re the jet velocity was doubled and, to negate its influence on Da, the preexponential factor $A$ was halved; to double optical thickness, the jet diameter was doubled while halving $u_j$ (to keep Re constant) and also adjusting $A$ (to keep Da constant), etc. For later identification the flames have been named and their nondimensional parameters have been summarized in Table 1.

To simulate these flames, a rectangular axisymmetric domain of $70 d_j \times 18 d_j$ was used, and a nonuniform grid system of $60 \times 70$ nodes was found fine enough to give grid-independent results in the finite volume code. The global time step in the PDF/particle code was varied between 2 and 8ms, depending on jet speed and dimension. For each simulation roughly 1100 iterations were required to achieve statistically steady state. To limit cpu time radiation was only considered after the 300th iteration, while close to steady state, after 500 iterations, time – as well as spatial – averaging was used to obtain mean scalar values. Using about 58,000 statistical particles each simulation required approximately 22 cpu hours on a four processor Silicon graphics O200 computer.

In order to study turbulence-radiation interactions, three different scenarios were considered for each flame. In the first radiation is completely ignored to assess its overall importance on the flame. In the second and third scenarios radiation is considered, using the models described in the previous section, but TRI are ignored and considered, respectively. By ignoring TRI, it is implied that the two unclosed terms $\langle k_m \rangle$ and $\langle k_m a_m I_b \rangle$ are evaluated based on cell means for temperature and concentrations (denoted as $\bar{k}_m$ and $\bar{k}_m \bar{a}_m \bar{I}_b$); when considering TRI, these terms are evaluated exactly.

Table 1. Summary of investigated flame scenarios.

| Flame | Re | $\kappa L$ | Da | Fr |
|---|---|---|---|---|
| Re.1 | 11200 | 0.474 | 1270 | $\infty$ |
| Re.2 | 22400 | 0.474 | 1270 | $\infty$ |
| Re.3 | 44800 | 0.474 | 1270 | $\infty$ |
| $\kappa L$.1 | 22400 | 0.237 | 317.5 | $\infty$ |
| $\kappa L$.2 | 22400 | 0.474 | 317.5 | $\infty$ |
| $\kappa L$.3 | 22400 | 0.948 | 317.5 | $\infty$ |
| Da.1 | 22400 | 0.474 | 317.5 | $\infty$ |
| Da.2 | 22400 | 0.474 | 1270 | $\infty$ |
| Da.3 | 22400 | 0.474 | $\infty$ | $\infty$ |
| Fr.1 | 22400 | 0.474 | 1270 | 0.358 |
| Fr.2 | 22400 | 0.474 | 1270 | 0.506 |
| Fr.3 | 22400 | 0.474 | 1270 | $\infty$ |
| Fr.4 | 22400 | 0.948 | 317.5 | 0.200 |
| Fr.5 | 22400 | 0.948 | 317.5 | 0.283 |
| Fr.6 | 22400 | 0.948 | 317.5 | $\infty$ |

## Influence of Flame Parameters on TRI

The importance of radiation, in general, and TRI, in particular, on a flame are manifested by their impact on (i) the temperature level of the flame, (ii) the "radiant fraction" and (iii) the local radiative source term, $\langle S^R \rangle$, which couples radiation to the overall energy equation. The radiative fraction is defined as the ratio of the net radiative heat loss from the flame to the total heat released during combustion, or

$$f_{\text{rad}} \equiv \frac{\dot{Q}_{\text{rad}}}{\dot{m}_{\text{fuel}} \Delta h_{\text{comb}}} \tag{29}$$

where $\Delta h_{\text{comb}}$ is the heat of combustion.

Typical temperature fields for the three scenarios are shown in Fig. 2, here for flame $\kappa L$.3. It is observed that considering radiation uniformly depresses the temperature level (due to radiative heat loss), and that accounting for TRI results in a further decrease (increasing radiative heat loss). While flame $\kappa L$.3 is fairly optically thick (with larger radiative emission and losses), the trends are the same for every flame, as indicated in Table 2, which compares peak flame temperatures, although the effects are strongest for larger optical thickness.

The effects of flame parameters on total emitted radiative energy, $\dot{Q}_{\text{em}}$, absorbed energy, $\dot{Q}_{\text{abs}}$, net radiative heat loss $\dot{Q}_{\text{net}} = \dot{Q}_{\text{em}} - \dot{Q}_{\text{abs}}$, and radiant fraction are summarized in Table 3. As a general trend it can be observed that TRI tend to increase radiative emission as well as absorption, except for flames with large optical thickness. This does not imply that optically thick flames encounter less TRI: for large values of $\tau_{\text{flame}}$ TRI strongly lowers the temperature level, thus significantly reducing non-TRI emission, and the increase in emission due to TRI barely makes up for this loss.

**Effects of Reynolds Number**. Studying the results of Tables 1 and 2 for the Re-series of flames

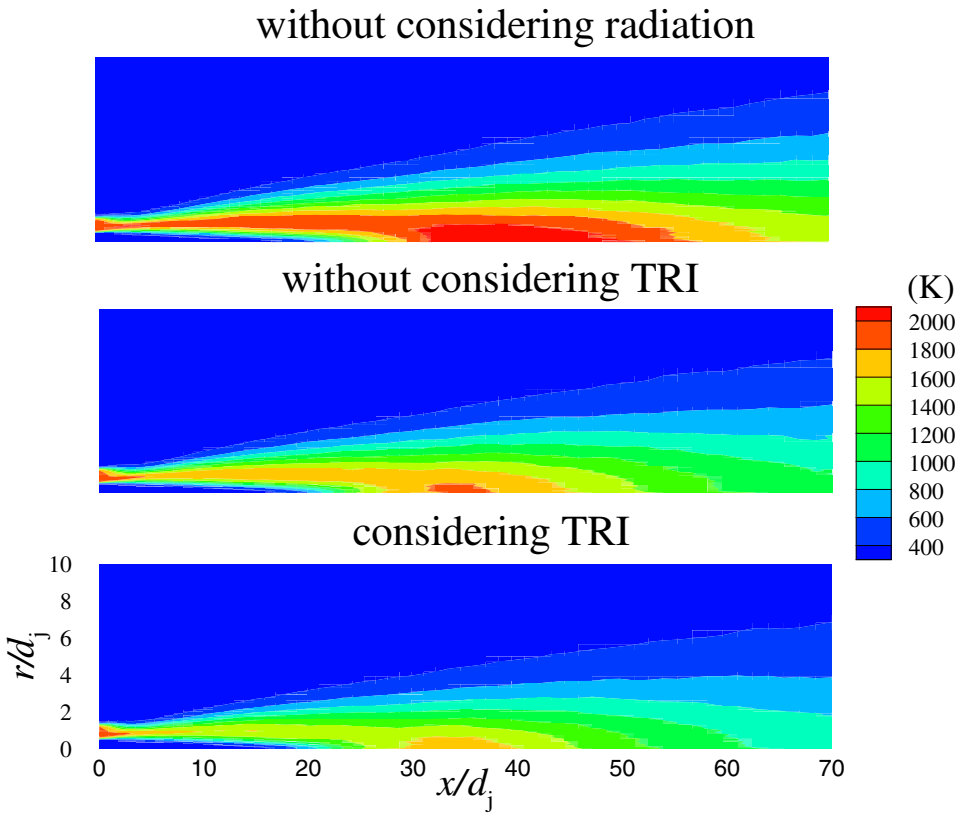


Figure 2. Temperature structure for Flames $\kappa L.3$

it is observed that flame temperature increases with Re, while the radiant fraction decreases. In these results the change in Re has been achieved by varying the jet velocity. Since flame length is only a function of jet diameter and not dependent on the jet velocity for momentum dominated flames with very fast chemistry [66], increasing Re then implies that the residence time of individual particles in the flame is decreased. This implies that the fluid particles have less time to radiate heat, increasing flame temperature and decreasing the radiant fraction. If Re is further increased the flame nears extinction and TRI can dramatically alter the flame's behavior: increasing Re to Re $= 100,000$ leads to a stable flame if TRI are ignored, but to complete extinction if TRI are considered (the lack of reaction then lowers temperature levels).

**Effects of Optical Thickness**. Optical thickness was varied by changing the jet diameter $d_j$. As the $\kappa L$-series of flames shows, optically thin flames have little self-absorption of radiative emission ($\dot{Q}_{\text{abs}}/\dot{Q}_{\text{em}} = 14\%$ for flame $\kappa L.1$ vs. $45\%$ for $\kappa L.3$), giving credence to the often-employed optically-thin radiation models employed for such flames (i.e., neglecting $\dot{Q}_{\text{abs}}$). However, TRI effects are strong, raising $\dot{Q}_{\text{em}}$ by almost 59% for flame $\kappa L.1$. The fact that $\dot{Q}_{\text{em}}$ does not increase, and may even decrease, for larger optical thickness is a function of the low flame temperature caused by large radiative heat loss, not by diminishing TRI. In the given study optical thickness was increased by increasing the size of the flame and, at the same time, increasing the residence time of fluid particles. This leads to larger radiation losses and lower temperatures (even though more of the emission is trapped within the flame by self-absorption). Again, there is an extinction limit, which depends on the TRI: in this series a $\tau_{\text{flame}} \simeq 1.185$ allows a flame to exist if TRI are

Table 2. Computed flame peak temperatures.

| Flames | $T_{\mathrm{norad}}$ (K) | $T_{\mathrm{noTRI}}$ (K) | $T_{\mathrm{TRI}}$ (K) | $\triangle T_{\mathrm{rad}}$ (K) | $\triangle T_{\mathrm{TRI}}$ (K) |
|---|---|---|---|---|---|
| Re.1 | 2181 | 1929 | 1869 | −252 | −60 |
| Re.2 | 2165 | 2018 | 1967 | −147 | −51 |
| Re.3 | 2173 | 2079 | 2047 | −94 | −32 |
| $\kappa L$.1 | 2165 | 2101 | 2083 | −64 | −18 |
| $\kappa L$.2 | 2161 | 2016 | 1952 | −145 | −64 |
| $\kappa L$.3 | 2169 | 1842 | 1725 | −327 | −117 |
| Da.1 | 2161 | 2016 | 1952 | −145 | −64 |
| Da.2 | 2165 | 2018 | 1967 | −147 | −51 |
| Da.3 | 2175 | 2005 | 1974 | −170 | −31 |
| Fr.1 | 2182 | 2013 | 1974 | −169 | −39 |
| Fr.2 | 2177 | 2016 | 1972 | −161 | −44 |
| Fr.3 | 2165 | 2018 | 1967 | −147 | −51 |
| Fr.4 | 2127 | 1840 | 1453 | −287 | −387 |
| Fr.5 | 2147 | 1820 | 1670 | −327 | −150 |
| Fr.6 | 2169 | 1842 | 1725 | −327 | −117 |

neglected, but it is extinguished if TRI are considered.

**Effects of Damköhler Number**. To study the effects of lowering the Damköhler number one can decrease the turbulent time scale by increasing the jet velocity, or on can increase the chemical reaction time scale by artificially lowering the reaction rate (by decreasing the preexponential factor). While the first may be more realistic, the second was chosen here, because in this way finite-rate effects can be isolated from other phenomena (i.e., one can hold Re, $\tau_{\mathrm{flame}}$ and Fr constant). Table 3 shows that lowering Da has only a minor effect on the radiation field, including TRI, increasing $\dot{Q}_{\mathrm{net}}$ and $f_{\mathrm{rad}}$ slightly as Da decreases. (A decreasing Da, however, has a strong effect on the flame structure: as Da decreases the reaction moves downstream leading to extinction. In this series of flames this occurs at $Da = 127$ if TRI are considered).

**Effects of Froude Number**. To study the effects of buoyancy on TRI the Froude number was varied by changing the gravitational acceleration $g$. Fr.1–Fr.3 correspond to fairly small flames, which are hardly at all affected by gravity: overall radiation levels decrease slightly, while the TRI are totally unaffected (increasing the radiant fraction by 2.5% for all Fr). In larger flames, Fr.4–Fr.6, buoyancy becomes an important driving force for turbulent mixing and a decreasing Froude number has an impact on flame structure and radiative heat loss, with radiant fraction dropping from 18.1% ($Fr = \infty$ or $g = 0$) to 10.2% ($Fr = 0.2$ or $g = 4$ m/s$^2$). If $g$ is further increased to 4.9 m/s$^2$ no flame exists.

**Separation of TRI Effects**. It was observed earlier that there is a strong feedback between TRI and overall emission: if TRI are strong this leads to a large decrease in temperature levels and, thus, "regular" emission, as clearly seen in flame $\kappa L$.3 (cf. Table 3). In order to separate TRI from overall emission, and to study various aspects of TRI, a set of "frozen particle field"

Table 3. Summary of radiation calculation results.

| Flame | Without TRI | | | | With TRI | | | |
|---|---|---|---|---|---|---|---|---|
| | $\dot{Q}_{\mathrm{em}}$ (kW) | $\dot{Q}_{\mathrm{abs}}$ (kW) | $\dot{Q}_{\mathrm{net}}$ (kW) | $f_{\mathrm{rad}}$ (%) | $\dot{Q}_{\mathrm{em}}$ (kW) | $\dot{Q}_{\mathrm{abs}}$ (kW) | $\dot{Q}_{\mathrm{net}}$ (kW) | $f_{\mathrm{rad}}$ (%) |
| Re.1 | 2.86 | 0.75 | 2.11 | 12.0 | 4.28 | 1.10 | 3.18 | 18.1 |
| Re.2 | 3.66 | 0.99 | 2.67 | 7.63 | 5.51 | 1.48 | 4.03 | 11.5 |
| Re.3 | 4.14 | 1.13 | 3.01 | 4.31 | 6.37 | 1.75 | 4.62 | 6.59 |
| $\kappa L$.1 | 0.597 | 0.081 | 0.516 | 2.94 | 0.928 | 0.130 | 0.798 | 4.56 |
| $\kappa L$.2 | 3.42 | 0.91 | 2.51 | 7.14 | 5.33 | 1.41 | 3.92 | 11.2 |
| $\kappa L$.3 | 12.77 | 5.14 | 7.63 | 10.9 | 20.94 | 8.26 | 12.68 | 18.1 |
| Da.1 | 3.42 | 0.91 | 2.51 | 7.14 | 5.33 | 1.41 | 3.92 | 11.2 |
| Da.2 | 3.66 | 0.99 | 2.67 | 7.63 | 5.51 | 1.48 | 4.03 | 11.5 |
| Da.3 | 4.02 | 1.11 | 2.91 | 8.31 | 5.72 | 1.57 | 4.15 | 11.8 |
| Fr.1 | 2.85 | 0.66 | 2.19 | 6.26 | 4.47 | 1.04 | 3.43 | 9.79 |
| Fr.2 | 3.16 | 0.78 | 2.38 | 6.79 | 4.86 | 1.20 | 3.66 | 10.4 |
| Fr.3 | 3.66 | 0.99 | 2.67 | 7.62 | 5.51 | 1.48 | 4.03 | 11.5 |
| Fr.4 | 4.67 | 1.17 | 3.50 | 5.00 | 9.81 | 2.63 | 7.18 | 10.2 |
| Fr.5 | 8.50 | 2.84 | 5.66 | 8.09 | 15.58 | 5.18 | 10.40 | 14.8 |
| Fr.6 | 12.77 | 5.14 | 7.63 | 10.9 | 20.94 | 8.26 | 12.68 | 18.1 |

studies were performed. In these studies fixed particle fields were taken from the fully converged solution (including the effects of TRI). These fixed fields (with fixed mean scalar fields) were then used to calculate the radiation from it with and without TRI. The results are tabulated in Table 4, clearly showing that the overall level of TRI is relatively unaffected by any of the nondimensional parameters, always being in the range from 50 to 60%. Thus, TRI can always be expected to be of great importance in flames of this class.

In order to find out which particular correlations dominate the TRI effects, several partial TRI scenarios were studied for the $\kappa L$-series of flames. Besides the cases of no TRI and full TRI four partial-TRI scenarios were also considered: in the first only the absorption coefficient self correlation in the absorption term is considered, (labeled $\langle\kappa\rangle$), while the emission components are individually evaluated at the mean temperature and concentrations (denoted by $\bar{\kappa}\bar{a}\bar{I}_b$ with the overbar meaning "evaluated at mean scalars"). In the second only the Planck function self correlation is considered, the rest evaluated at mean scalars (i.e., $\bar{\kappa}$ for absorption and $\bar{\kappa}\bar{a}\,\langle I_b\rangle$ for emission); the third considers the spectrally weighted Planck function $\langle aI_b\rangle$ (i.e., $\bar{\kappa}$ for absorption, $\bar{\kappa}\,\langle aI_b\rangle$ for emission); finally, the fourth treats the fluctuations of the entire emission term (i.e., $\bar{\kappa}$ for absorption and $\langle\kappa aI_b\rangle$ for emission). The results are summarized in Table 5.

*Effects of* $\langle\kappa\rangle$. It is observed that considering the fluctuations of the absorption coefficient always increases absorption, but this increase is quite small, ranging from 4% ($\kappa L$.3) to 10% ($\kappa L$.1), indicating that exact treatment of this term is of minor importance. This was to be expected since $\kappa_\eta$ is essentially linearly dependent on concentrations and, for the range of typical fluctuations, almost linear in temperature.

Table 4. Effects of TRI on radiant fractions for fixed temperature field

| Flame | $f_{\text{rad}}$, (%) | | $\frac{f_{\text{rad}}^{\text{TRI}} - f_{\text{rad}}^{\text{noTRI}}}{f_{\text{rad}}^{\text{noTRI}}}$ (%) |
|---|---|---|---|
| | withoutTRI | withTRI | |
| Re.1 | 12.0 | 18.1 | 51 |
| Re.2 | 7.63 | 11.5 | 51 |
| Re.3 | 4.31 | 6.59 | 53 |
| $\kappa L$.1 | 2.94 | 4.56 | 55 |
| $\kappa L$.2 | 7.14 | 11.2 | 57 |
| $\kappa L$.3 | 10.9 | 18.1 | 66 |
| Da.1 | 7.14 | 11.2 | 57 |
| Da.2 | 7.63 | 11.5 | 51 |
| Da.3 | 8.31 | 11.8 | 42 |
| Fr.1 | 6.26 | 9.79 | 56 |
| Fr.2 | 6.79 | 10.4 | 53 |
| Fr.3 | 7.62 | 11.5 | 51 |
| Fr.4 | 5.00 | 10.2 | 104 |
| Fr.5 | 8.09 | 14.8 | 83 |
| Fr.6 | 10.9 | 18.1 | 66 |

*Effects of* $\langle I_b \rangle$ *and* $\langle aI_b \rangle$. It has been asserted in some early work that, due to its strong nonlinearity, the Planck function self correlation $\langle I_b \rangle$ should dominate the TRI contributions. Indeed, consideration of $\langle I_b \rangle$ alone increases emission and net radiation loss by about one third for all three flames. However, this argument only holds for gray media (the object of early studies); if the nongrayness of combustion gases is considered, $\langle aI_b \rangle$, the effective Planck function (integrated only over gas absorption bands) is much less nonlinear in temperature. For nongray gases the emission term increases by only about 7% ($\kappa L$.1) to 12% ($\kappa L$.3), about the same as the absorption coefficient self correlation. This leads to the important conclusion that TRI effects have a lesser impact on nongray media than on gray ones.

Effects of $\langle \kappa aI_b \rangle$. Consideration of the correlation between nongray absorption coefficient and the Planck function turns out to be by far the most important, increasing emission by 55% ($\kappa L$.1 and $\kappa L$.2) to 65% ($\kappa L$.3). It is interesting to note that, while the absorption coefficient self correlation $\langle \kappa \rangle$ and nongray Planck function self correlation $\langle aI_b \rangle$ are individually not of great importance, the positive correlation between them makes the absorption coefficient–Planck function correlation dominant.

# DNS Calculations of TRI

Since PDF simulations include a number of modeled (i.e., approximate) terms, their accuracy must be verified, and this is most conveniently done through direct numerical simulation (DNS). In addition, PDF methods in general use simplified RTE solvers, which cannot resolve the absorption

Table 5. Comparison of TRI components for series of $\kappa L$-flames

| $k$-correlation | | $\bar{k}$ | $\langle k\rangle$ | $\bar{k}$ | $\bar{k}$ | $\bar{k}$ | $\langle k\rangle$ |
|---|---|---|---|---|---|---|---|
| $kaI_b$-correlation | | $\bar{k}\bar{a}\bar{I}_b$ | $\bar{k}\bar{a}\bar{I}_b$ | $\bar{k}\bar{a}\langle I_b\rangle$ | $\bar{k}\langle aI_b\rangle$ | $\langle kaI_b\rangle$ | $\langle kaI_b\rangle$ |
| $\kappa L.1$ | $\dot{Q}_{\rm em}$ (kW) | 0.597 | 0.597 | 0.812 | 0.641 | 0.928 | 0.928 |
| | $\dot{Q}_{\rm abs}$(kW) | 0.082 | 0.090 | 0.106 | 0.086 | 0.118 | 0.130 |
| | $\dot{Q}_{\rm net}$(kW) | 0.516 | 0.507 | 0.706 | 0.555 | 0.820 | 0.798 |
| | $f$ (%) | 2.94 | 2.90 | 4.03 | 3.17 | 4.68 | 4.56 |
| $\kappa L.2$ | $\dot{Q}_{\rm em}$ (kW) | 3.42 | 3.42 | 4.59 | 3.69 | 5.33 | 5.33 |
| | $\dot{Q}_{\rm abs}$(kW) | 0.904 | 0.965 | 1.17 | 0.960 | 1.32 | 1.41 |
| | $\dot{Q}_{\rm net}$(kW) | 2.51 | 2.45 | 3.42 | 2.73 | 4.02 | 3.92 |
| | $f$ (%) | 7.14 | 6.98 | 9.74 | 7.78 | 11.5 | 11.2 |
| $\kappa L.3$ | $\dot{Q}_{\rm em}$ (kW) | 12.7 | 12.7 | 17.5 | 14.2 | 20.9 | 20.9 |
| | $\dot{Q}_{\rm abs}$(kW) | 5.13 | 5.33 | 6.80 | 5.62 | 7.97 | 8.26 |
| | $\dot{Q}_{\rm net}$(kW) | 7.63 | 7.44 | 10.6 | 8.63 | 13.1 | 12.7 |
| | $f$ (%) | 10.9 | 10.6 | 15.1 | 12.3 | 18.7 | 18.1 |

coefficient–intensity correlation $\langle\kappa I\rangle$ (an exception being the recent work by Tessé et al. [33], who used a complicated Monte Carlo scheme to capture TRI, including $\langle\kappa I\rangle$). Thus, DNS simulations can also be used to quantify $\langle\kappa I\rangle$ and test the accuracy of the optically thin eddy assumption (OTFA). As indicated earlier, Wu et al. [36, 37] considered a one-dimensional flame with single-step finite-rate Arrhenius chemistry (in terms of temperature and a simple progress variable). The underlying DNS code uses third order Runge-Kutta time integration, and a sixth-order compact scheme for spatial discretization. To obtain the radiative source term for the energy equation a high-order photon Monte Carlo scheme was developed, commensurate with the order of the underlying DNS code. Emission and absorption of photon bundles, using the energy partitioning method [39], is done via an adaptive scheme, which uses up to sixth-order polynomials in regions of strong gradients. In these early studies only a gray, nonscattering medium is considered with a temperature and progress variable dependent Planck-mean absorption coefficient, fashioned after the water vapor model suggested by [21]. For the cases studied radiation required about ten times the CPU time of the underlying simple-chemistry DNS code. Once nongray gases will be modeled (say, with the FSK model), the radiation effort can be expected to grow about tenfold. On the other hand, if detailed chemistry is to be considered on may expect the DNS calculations to dominate the CPU requirements (and demanding a computer of great power). Four different flames where considered, the first three were calculated on a 2D $451 \times 451$ grid, with varying optical thickness $\kappa_{\rho,2} l_{11}$ (based on burned-gas properties and initial turbulence integral length scale) of 0.1 (Case 1), 1 (Case 2) and 10 (Case 3); the fourth flame is calculated on a $144^3$ 3D grid with $\kappa_{\rho,2} l_{11} = 1$ (Case 4).

The absorption coefficient–Planck function correlation $\langle\kappa I_b\rangle/\langle\kappa\rangle\langle I_b\rangle$ is shown in Fig. 3. For the three two-dimensional cases (Cases 1–3) the values for these nondimensional quantities are essentially the same for all values of optical thickness. This is a direct consequence of the fact that the values of $\kappa_P(Y_\rho, T)$ for these cases differ simply by a multiplicative constant (larger differences

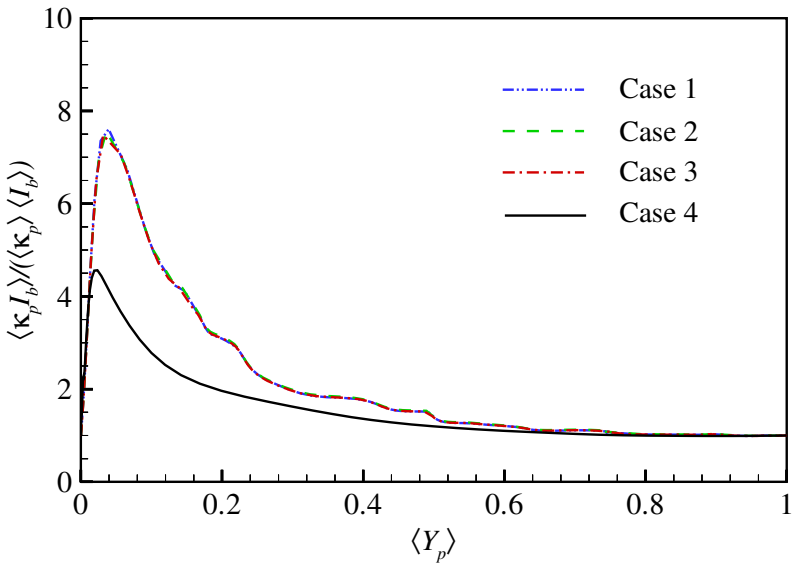


Figure 3. Absorption coefficient–Planck function correlation vs. mean progress variable from 2D and 3D DNS calculations.

resulted when different functional forms were used for $\kappa_P$). The three-dimensional case is qualitatively similar to the other cases. Absorption TRI is examined in Fig. 4. The OTFA approximation of $\langle \kappa_P G \rangle \simeq \langle \kappa_P \rangle \langle G \rangle$ improves with decreasing optical thickness, as expected. However, even in the most optically thin case examined the ratio ranges from 0.8 to 1.1 through the flame brush. Again, three-dimensional results (Case 4) are similar to the corresponding 2D case (Case 2).

The DNS results presented here are very preliminary and use a highly idealized model. Qualitatively, however, they nicely complement and corroborate the PDF model conclusions. For a meaningful comparison it must be remembered that Figs. 3 and 4 show *local* TRI correlation values, while those given in Tables 2 and 4 are flame averages.

# Summary and Conclusions

In this paper the state-of-the-art of modeling turbulence-radiation interactions, with their vast ranges of length scales and time scales, was reviewed. Special emphasis was given to methods that can resolve all necessary scales from basic principles, such as the composition PDF method and DNS calculations. Some pertinent results were given and the relative importance of the different components constituting the TRI were assessed. It was found that the Planck function self-correlation $\langle I_b \rangle$ is an important (but not dominating) contributor in gray media, but much less so in nongray combustion gases. In general, TRI are dominated by the correlation between absorption coefficient and Planck function $\langle \kappa I_b \rangle$. DNS calculations have verified the applicability of the commonly used optically thin fluctuation assumption (OTFA), although locally the absorption coefficient–intensity correlation $\langle \kappa I \rangle$ is never quite negligible.

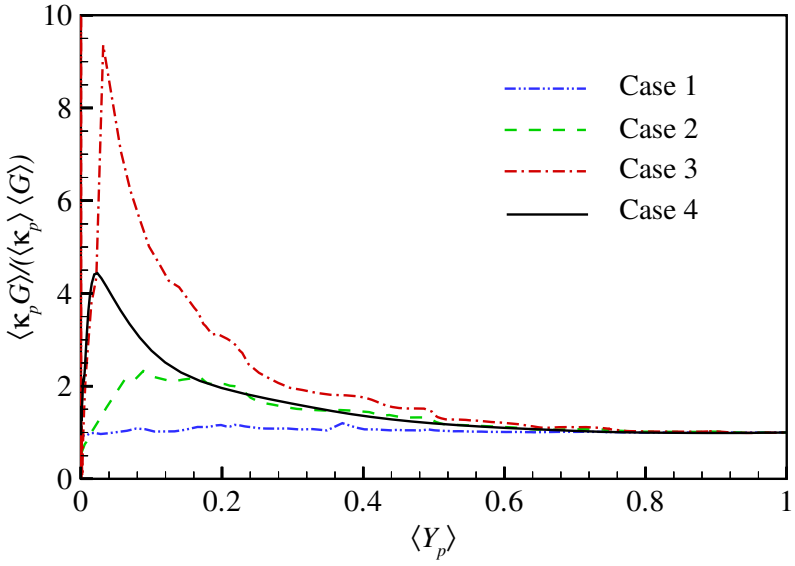


Figure 4. Absorption coefficient–incident radiation correlation vs. mean progress variable from 2D and 3D DNS calculations.

# References


[1] Bilger, R. W., 1989, "Turbulent diffusion flames", *Ann. Rev. Fluid Mech.*, **21**, pp. 101–135.

[2] Bilger, R. W., 2000, "Future Progress in Turbulent Combustion Research", *Progress in Energy and Combustion Science*, **26**, pp. 367–380.

[3] Townsend, A. A., 1958, "The Effects of Radiative Transfer on Turbulent Flow of a Stratified Fluid", *Journal of Fluid Mechanics*, **4**, pp. 361–375.

[4] Shved, G. M. and Akmayev, R. A., 1977, "Influence of Radiative Heat Transfer on Turbulence in Planetary Atmospheres", *Atmos. and Oceanic Phys.*, **34**, pp. 1286–1401.

[5] Song, T. H. and Viskanta, R., 1987, "Interaction of Radiation with Turbulence: Application to a Combustion System", *Journal of Thermophysics and Heat Transfer*, **1**(1), pp. 56–62.

[6] Soufiani, A., Mignon, P., and Taine, J., 1990, "Radiation–Turbulence Interaction in Channel Flows of Infrared Active Gases", In *Proceedings of the Ninth International Heat Transfer Conference*, **6**, Washington, D.C., Hemisphere, pp. 403–408.

[7] Hall, R. J. and Vranos, A., 1994, "Efficient Calculations of Gas Radiation From Turnbulent Flames", *International Journal of Heat and Mass Transfer*, **37**, p. 2745.

[8] Mazumder, S. and Modest, M. F., 1999, "A PDF Approach to Modeling Turbulence–Radiation Interactions in Nonluminous Flames", *International Journal of Heat and Mass Transfer*, **42**, pp. 971–991.

[9] Viskanta, R., 1998, "Overview of Convection and Radiation in High Temperature Gas Flows", *International Journal of Engineering Science*, **36**, pp. 1677–1699.

[10] Faeth, G. M., Gore, J. P., Chuech, S. G., and Jeng, S. M., 1989, "Radiation from Turbulent Diffusion Flames", In *Annual Review of Numerical Fluid Mechanics and Heat Transfer*, **2**, Hemisphere, Washington, D.C., pp. 1–38.

[11] Cox, G., 1977, "On Radiant Heat Transfer from Turbulent Flames", *Combustion Science and Technology*, **17**, pp. 75–78.

[12] Germano, M., 1978, "Turbulent Fluctuations Coupled with the Radiation Field", AIAA Paper No. 78-840.

[13] Pearce, B. and Varma, A., 1981, "Radiation–Turbulence Interaction in a Tactical Missile Exhaust Plume", *AIAA Paper, No. 81-1110*.

[14] Chan, S. H. and Chern, C. F., 1990, "A Method for Turbulence–Radiation Interaction Analysis in Multiphase Liquid Metal Diffusion Flames", In *Proceedings of the Ninth International Heat Transfer Conference*, **4**, Washington, D.C., Hemisphere, pp. 143–148.

[15] Mukerji, S., McDonough, J. M., Mengüç, M. P., Manickavasagam, S., and Chung, S., 1998, "Chaotic Map Models Of Soot Fluctuations In Turbulent Diffusion Flames", *International Journal of Heat and Mass Transfer*, **41**(24), pp. 4095–4112.

[16] Xu, Y., McDonough, J. M., and Mengüç, M. P., 2002, "Turbulence-radiation interactions in flames: A chaotic-map based formulation", In *Proceedings of the 2002 IMECE*, ASME.

[17] Gore, J. P., Ip, U.-S., and Sivathanu, Y. R., 1992, "Coupled Structure and Radiation Analysis of Acetylene/Air Flames", *ASME Journal of Heat Transfer*, **114**, pp. 487–493.

[18] Hartick, J. W., Tacke, M., Fruchtel, G., Hassel, E. P., and Janicka, J., 1996, "Interaction of Turbulence and Radiation in Confined Diffusion Flames", In *Twenty-Sixth Symposium (International) on Combustion*, The Combustion Institute, pp. 75–82.

[19] Ripoll, J.-F., 2004, "An averaged formulation of the $M_1$ radiation model with mean absorption coefficients and presumed probability density functions for turbulent flows", *Journal of Quantitative Spectroscopy and Radiative Transfer*, **83**, pp. 493–517.

[20] Coelho, P. J., Teerling, O. J., and Roekaerts, D., 2003, "Spectral radiative effects and turbulence/radiation interaction in a non-luminous turbulent jet diffusion flame", *Combustion and Flame*, **133**, pp. 75–91.

[21] See http://www.ca.sandia.gov/tdf/Workshop.html.

[22] Snegirev, A. Y., 2004, "Statistical modeling of thermal radiation transfer in buoyant turbulent diffusion flames", *Combustion and Flame*, **136**, pp. 51–71.

[23] Souil, J. M., Joulain, P., and Gengembre, E., 1984, *Combustion Science and Technology*, **41**, pp. 69–81.

[24] Pope, S. B., 1985, "PDF Methods for Turbulent Reactive Flows", *Progress in Energy and Combustion Science*, **11**, pp. 119–192.

[25] Kollmann, W., 1990, "The PDF Approach to Turbulent Flow", *Theor. Compt. Fluid Dyn.*, **1**, pp. 249–285.

[26] Dopazo, C., 1994, "Recent developments in pdf methods", In *Turbulent Reacting Flows*, Academic Press, pp. 375–474.

[27] Raman, V., Fox, R. O., and Harvey, A. D., 2004, "Hybrid finite-volume/transported PDF simulations of a partially premixed methane–air flame", *Combustion and Flame*, **136**, pp. 327–350.

[28] Mazumder, S. and Modest, M. F., 1999, "A PDF Approach to Modeling Turbulence–Radiation Interactions in Nonluminous Flames", *International Journal of Heat and Mass Transfer*, **42**, pp. 971–991.

[29] Subramaniam, S. V. and Haworth, D. C., 2000, "A PDF Method for Turbulent Mixing and Combustion on Three-Dimensional Unstructured Deforming Meshes", *Intern'l. J. Engine Research*, **1**, pp. 171–190.

[30] Li, G. and Modest, M. F., 2002, "Application of composition PDF methods in the investigation of turbulence–radiation interactions", *Journal of Quantitative Spectroscopy and Radiative Transfer*, **73**, pp. 461–472.

[31] Li, G. and Modest, M. F., 2003, "Importance of Turbulence–Radiation Interactions in Turbulent Diffusion Jet Flames", *ASME Journal of Heat Transfer*, **125**, pp. 831–838.

[32] Modest, M. F., 2003, "Narrow-band and full-spectrum *k*-distributions for radiative heat transfer—correlated-*k* vs. scaling approximation", *Journal of Quantitative Spectroscopy and Radiative Transfer*, **76**(1), pp. 69–83.

[33] Tessé, L., Dupoirieux, F., and Taine, J., 2004, "Monte Carlo modeling of radiative transfer in a turbulent sooty flame", *International Journal of Heat and Mass Transfer*, **47**, pp. 555–572.

[34] Coelho, P. J., 2004, "Detailed numerical simulation of radiative transfer in a nonluminous turbulent jet diffusion flame", *Combustion and Flame*, **136**, pp. 481–492.

[35] Chan, S. H. and Pan, X. C., 1997, "A General Semicausal Stochastic Model for Turbulence/Radiation Interactions in Flames", *ASME Journal of Heat Transfer*, **119**(3), pp. 509–516.

[36] Wu, Y., Haworth., D. C., Modest, M. F., and Cuenot, B., 2004, "Direct Numerical Simulation of Turbulence/Radiation Interaction in Premixed Combustion Systems", In *Thirtyeth Symposium (International) on Combustion*, The Combustion Institute.

[37] Wu, Y., Modest, M. F., and Haworth., D. C., 2004, "Development of a photon Monte Carlo method for DNS of chemically reacting turbulent flows", *Combustion Theory and Modeling*, in preparation.

[38] Kuo, K. K., 1986, *Principles of Combustion*, Wiley Interscience, New York.

[39] Modest, M. F., 2003, *Radiative Heat Transfer*, Academic Press, New York, 2nd ed.

[40] Kabashinikov, V. P. and Myasnikova, G. I., 1985, "Thermal Radiation in Turbulent Flows—Temperature and Concentration Fluctuations", *Heat Transfer-Soviet Research*, **17**(6), pp. 116–125.

[41] Dopazo, C., 1975, "Probability density function approach for a turbulent axisymmetric heated jet. Centerline evolution", *Physics of Fluids*, **18**, pp. 397–404.

[42] Tsai, K. and Fox, R. O., 1998, "The BMC/GIEM Model for Micromixing in Non-Premixed Turbulent Reacting Flows", *Ind. Eng. Chem. Res.*, **37**, pp. 2131–2141.

[43] Subramaniam, S. and Pope, S. B., 1999, "Comparison of mixing model performance for nonpremixed turbulent reactive flow", *Combustion and Flame*, **117**, pp. 732–754.

[44] Ren, Z. and Pope, S. B., 2004, "An investigation of the performance of turbulent mixing models", *Combustion and Flame*, **136**, pp. 208–216.

[45] Janicka, J., Kolbe, W., and Kollmann, W., 1978, "The Solution of a PDF-Transport Equation for Turbulent Diffusion Flames", In *Proceedings of 1978 Heat Trans. Fluid Mech. Inst., Stanford University*.

[46] 1998, *FLUENT Computational Fluid Dynamics Software*, Version 5, Fluent Corp., New Hampshire.

[47] Li, G. and Modest, M. F., 2001, "An Effective Particle Tracing Scheme on Structured/Unstructured Grids in Hybrid Finite Volume/PDF Monte Carlo Methods", *Journal of Computational Physics*, **173**, pp. 187–207.

[48] Westbrook, C. K. and Dryer, F. L., 1981, "Simplified Reaction Mechanisms for the Oxidation of Hydrocarbon Fuels in Flames", *Combustion Science and Technology*, **27**, pp. 31–43.

[49] Pope, S. B., 1997, "Computationally Efficient Implementation of Combustion Chemistry Using in situ Adaptive Tabulation", *Combust. Theory& Modeling*, **1**, pp. 41–63.

[50] Veljkovic, Ivana, Plassmann, Paul, and Haworth, Daniel, 2003, "A Scientific On-Line Database for Efficient Function Approximation", In *Computational Science and Its Applications—ICCSA 2003, The Springer Verlag Lecture Notes in Computer Science (LNCS 2667), Part I.*

[51] Veljkovic, Ivana, Plassmann, Paul, and Haworth, Daniel, 2004, "A Parallel Implementation of Scientific On-Line Database for Efficient Function Approximation", In *Proceedings of the Conference on Parallel and Distributed Processing Techniques and Applications (PDPTA'04).*

[52] Hottel, H. C. and Sarofim, A. F., 1967, *Radiative Transfer*, McGraw-Hill, New York.

[53] Modest, M. F., 1991, "The Weighted-Sum-of-Gray-Gases Model for Arbitrary Solution Methods in Radiative Transfer", *ASME Journal of Heat Transfer*, **113**(3), pp. 650–656.

[54] Denison, M. K. and Webb, B. W., 1993, "An Absorption-Line Blackbody Distribution Function for Efficient Calculation of Total Gas Radiative Transfer", *Journal of Quantitative Spectroscopy and Radiative Transfer*, **50**, pp. 499–510.

[55] Denison, M. K. and Webb, B. W., 1993, "A Spectral Line Based Weighted-Sum-of-Gray-gases Model for Arbitrary RTE Solvers", *ASME Journal of Heat Transfer*, **115**, pp. 1004–1012.

[56] Rivière, Ph., Soufiani, A., Perrin, M. Y., Riad, H., and Gleizes, A., 1996, "Air Mixture Radiative Property Modelling in the Temperature Range 10000–40000 K", *Journal of Quantitative Spectroscopy and Radiative Transfer*, **56**, pp. 29–45.

[57] Pierrot, L., Soufiani, A., and Taine, J., 1999, "Accuracy of Narrow-band and Global Models for Radiative Transfer in $H_2O$, $CO_2$, and $H_2O$–$CO_2$ Mixtures at High Temperature", *Journal of Quantitative Spectroscopy and Radiative Transfer*, **62**, pp. 523–548.

[58] Rothman, L. S., Rinsland, C. P., Goldman, A., Massie, S. T., Edwards, D. P., Flaud, J.-M., Perrin, A., Camy-Peyret, C., Dana, V., Mandin, J.-Y., Schroeder, J., McCann, A., Gamache, R. R., Wattson, R. B., Yoshino, K., Chance, K. V., Jucks, K. W., Brown, L. R., Nemtchinov, V., and Varanasi, P., 1998, "The HITRAN Molecular Spectroscopic Database and HAWKS (HITRAN Atmospheric Workstation): 1996 Edition", *Journal of Quantitative Spectroscopy and Radiative Transfer*, **60**, pp. 665–710.

[59] Rothman, L. S., Camy-Peyret, C., Flaud, J.-M., Gamache, R. R., Goldman, A., Goorvitch, D., Hawkins, R. L., Schroeder, J., Selby, J. E. A., and Wattson, R. B., 2000, "HITEMP, the High-Temperature Molecular Spectroscopic Database", available through `http://www.hitran.com`.

[60] Modest, M. F. and Zhang, H., 2002, "The Full-Spectrum Correlated-*k* Distribution For Thermal Radiation from Molecular Gas–Particulate Mixtures", *ASME Journal of Heat Transfer*, **124**(1), pp. 30–38.

[61] Modest, M. F., 2003, "Backward Monte Carlo Simulations in Radiative Heat Transfer", *ASME Journal of Heat Transfer*, **125**(1), pp. 57–62.

[62] Li, G., 2002, *Investigation of Turbulence–Radiation Interactions By a Hybrid FV/PDF Monte Carlo Method*, PhD thesis, The Pennsylvania State University, University Park, PA.

[63] Li, G. and Modest, M. F., 2002, "Investigation of Turbulence–Radiation Interactions in Reacting Flows Using a Hybrid FV/PDF Monte Carlo Method", *Journal of Quantitative Spectroscopy and Radiative Transfer*, **73**(2–5), pp. 461–472.

[64] Li, G. and Modest, M. F., 2003, "Importance of Turbulence–Radiation Interactions in Turbulent Diffusion Jet Flames", *ASME Journal of Heat Transfer*, **125**, pp. 831–838.

[65] Li, G. and Modest, M. F., 2004, "Numerical simulation of turbulence-radiation interactions in turbulent reacting flows", In Sunden, B. and Faghri, M., eds., *Modelling and Simulation of Turbulent Heat Transfer*, WIT Press, Southampton, England.

[66] Turns, S. R., 2000, *An Introduction to Combustion: Concepts and Applications*, McGraw-Hill, 2nd ed.